PHYSICS

Iran J Radiol. 2019 January; 16(1):e13383. doi: 10.5812/iranjradiol.13383.

Published online 2018 September 18. **Research Article**

Investigating the Effect of mA Variation on Absorbed Dose to Salivary Glands and Mandible Body in CBCT

Zahra Alirezaei [1,*], Keyvan Jabbari [1], Tohid Dehghani [1], Mohammadbagher Tavakoli [1], Mojdeh Mehdizadeh [2], Nafiseh Berenjkoob [1] and Reihane Faraji [1]

[1] Department of Medical Physics, Isfahan University of Medical Sciences, Isfahan, Iran
[2] Department of Oral and Maxillofacial Radiology, School of Dentistry, Isfahan University of Medical Sciences, Isfahan, Iran

[*] *Corresponding author*: Department of Medical Physics, Isfahan University of Medical Sciences, Isfahan, Iran. Tel: +98-3137888191, Email: zahra.alirezaei@gmail.com

Received 2017 May 15; **Revised** 2018 August 11; **Accepted** 2018 August 18.

Abstract

Background: Cone beam computed tomography (CBCT) has been broadly acceptable in recent years as a radiography modality for diagnosis, treatment planning and follow up in dentistry. Some important parameters such as radiation dose, image quality and field of view are considered as a criteria for deciding whether or not a CBCT dental unit is suitable for a particular application.
Objectives: This study aims to evaluate the effect of exposure levels on the absorbed dose of mandible and salivary glands according to various settings of milliamperage (mA) in CBCT.
Materials and Methods: A very advanced multilayers head and neck phantom was constructed for this study. This phantom was built based on the CT images of a specific patient with an average size. This phantom was constructed using proper substitutes for soft tissue and bone according to their physical properties. Therefore, there was a high level of agreement with the patient's body. This phantom enables us to measure the absorbed dose inside the organs. Dosimetry has been performed by Soredex Cranex3d CBCT. For film dosimetry, AGFA films were used in various layers of the phantom. The mAs of the device was changed in the range of 2, 4, 6, 8, 10 and 12 mA.
Results: The maximum and the minimum absorbed dose was placed in the area related to the right mandible and the left submandibular gland. The increase of absorbed dose by mA increase was meaningful in the confidence level of 95% for all scanned areas. By changing mA from 2 to 12, the absorbed dose varied significantly with a maximum 5.44-fold variation between the highest and lowest dose for the parotid gland.
Conclusion: This study has shown that there is a meaningful relationship between the increase of mA and increase of absorbed dose in different parts of the dentomaxillofacial area, including the mandible, submandibular and parotid glands. It is concluded that as long as the image quality is acceptable for diagnostic purposes, the mAs of the CBCT should be kept in a low range to minimize the absorbed dose.

Keywords: Absorbed Dose, CBCT, Radiation Setting, Head Phantom

1. Background

Currently, cone beam computed tomography (CBCT) is an acceptable dental imaging modality used for every field in dentistry including implant planning, orthodontics, and maxillofacial surgery (1). Compared to other dental imaging techniques, CBCT has great advantages such as excellent spatial resolution, overlap of teeth, and acquisitioning three dimensional (3D) volumes of dental arches and surrounding tissues (2, 3).

In addition, images obtained from CBCT have excellent tissue contrast due to eliminating blurring and provide orthogonal views by reducing projection effects (4). CBCT has further advantages such as cost beneficience and considerably reduced effective radiation dose compared to regular CT (5).

While CBCT has the capability of producing 3D images with significantly less radiation than conventional CT, settings of the device plays a key role in the resulting radiation dose. The setting parameters include kilovoltage peak (kVp) and milliamperage (mA) (6, 7).

Previous studies have shown that both the lower and the higher exposure settings in medical CT units result in acceptable image quality (6-10). Although conventional dental imaging modalities still deliver lower radiation doses to patients, for some special cases in orthodontic treatment planning, undoubtedly a CBCT is preferred over a CT image (8).

Ludlow and co-workers found that as a dose sparing technique, dental CBCT is recommended compared to standard clinical scans for dental and maxillofacial radiographic imaging. Effective dose of standard scan of dental protocol (International Commission on Radiological Protection [ICRP]-2007) with multidetector computed tomography (MDCT) 1.5 to 3 times greater than that of using dental CBCT with average field (8).

Pauwels and co-workers showed that the dose for different organs varies in a wide range of value because of several factors such as radiation exposure setting, characteristics of primary beam and beam positioning respect to sensitive organs (9).

In another study, Pauwels and co-workers tried to optimize the kVp setting for a particular CBCT. They found that with the highest available kVp setting, the most optimal contrast is achievable at a fixed dose. There was a great potential for dose reduction through mA with a minimal loss in image quality (11).

Palomo and co-workers investigated various exposure settings, filters, and different collimation, and they found that lower settings and using the available collimation options a result in reduction in radiation dose (12).

In recent years, the number of accessible CBCT units has increased and new models have continuously been established. These devices cover a wide-ranging variability in terms of essential setting parameters including kVp, mA, filtration, and field of view. In addition, there is a degree of possibility in many devices for selecting certain exposure factors. The amount of absorbed dose in organs and the image quality for each scan depends on the type of device and imaging protocols. Radiation dose and image quality with the field of view are important factors by which the satisfaction of a certain CBCT unit can be determined regarding to the "as low as reasonably achievable" (ALARA) principle (13, 14).

To determine the risk of radiation for patients from X-ray imaging modalities, the effective dose is the preferable parameter over other alternatives (15-18). In dosimetry, it is impossible to directly place any kind of dosimeter inside an internal organ of body. Therefore, in order to measure the effective dose, an anthropomorphic phantom representing of an average human is frequently used (19).

2. Objectives

In the present study, we aimed to evaluate the effect of mA variation on the absorbed dose of the mandible and salivary glands according to various values of mA routinely used in CBCT.

3. Materials and Methods

In this study, a two dimensional film dosimetry method is represented by using radiographic film, and using the head phantom the effect of different milliamparages has been investigated on the distribution and amount of the received dose.

3.1. Phantom Construction

In this study, the measurements were performed by using a head phantom made of soft tissue-equivalent materials. The tissue-equivalent substitutes used for the phantom should meet two goals: similar physical properties to human tissue, such as density and attenuation coefficients, and simplicity of integration into the phantom construction process (20). A urethane-based resin was used to simulate the X-ray attenuation and density of human soft tissue. Another material combined from urethane-based and calcium carbonate ($CaCO_3$) was used to match human bone tissue within the diagnostic energy range (80 -120 kVp) (21).

Various factors were considered for designing and constructing the phantom. Regarding jaw dimension, teeth positioning and other segments of the dentomaxilla area, phantom designing was performed considering capability of dosimetry within mentioned situations in two parts including the head and jaw. The phantom was designed based on actual axial sections of a patient CT scan. Therefore, the geometry of each structure was matched accurately to the real head and radiological image of the phantom had great precision (21).

In the first step, we created a 3D file from CT scan images of a normal patient using 3D-Doctor software. Then, we extracted some parts of the maxillofacial area in Rhino software and a 3D file compatible to carbon dioxide laser (Co2-laser) machine was created and cut from perspex as soft tissue material. Bone equivalent material was a combination of a polyurethane based resin and $CaCo_3$ that was prepared using a laboratory mixer. At last we used some simple tools to embed this material in the desired segments (21). Figure 1 shows the slices of the phantoms in which equivalent bone material was embedded and the completed head phantom.

The selected areas for dosimetry were the sections in which the parotid gland, submandibular gland, and mandibular bone were placed. To achieve this goal, the precise locations of bones were determined so that the difference in the absorbed radiation dose between soft tissue and bone was clear. It should be noted that all slices of the phantom were prepared using automatic laser cutter. This laser cutter was moved along the border of the organ which was imported to the software. The imported data to

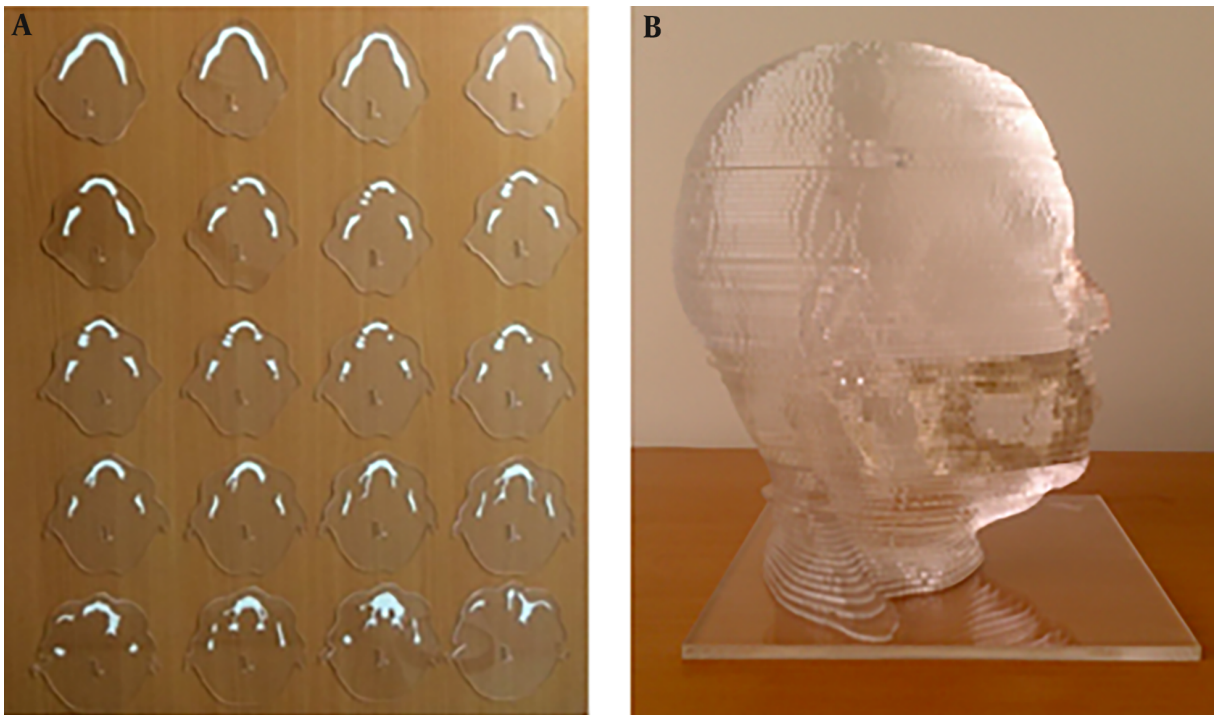

Figure 1. A, The slices of the phantom in which bone equivalent material was embedded, B, The constructed phantom using perspex and urethane-based resin.

software were derived from the CT scan of the patient directly. Finally, the constructed phantom was imaged by a Siemens 16-slices CT scanner in order to obtain Hounsfield unit measurements of the equivalent soft and bone tissues (Figure 2). The obtained Hounsfield units were 38 and 902 respectively which was in good agreement with real soft and bone tissue.

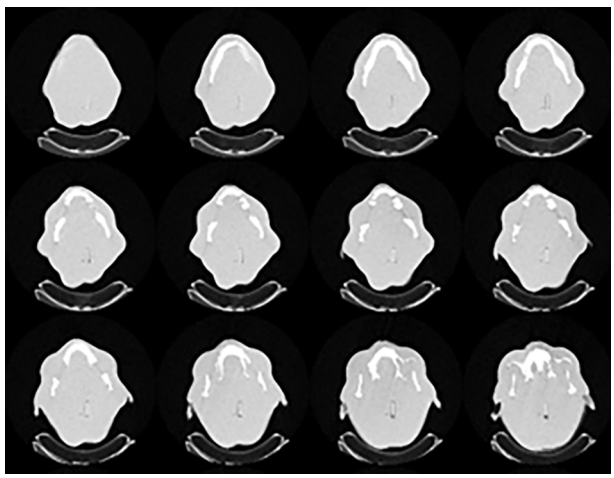

Figure 2. CT scan of some slices of the constructed phantom

3.2. Dosimetry

In this study, a radiographic film (AGFA ORTHO CP-GU) was used for evaluating the dose distribution in the phantom. This film is suitable for measurements of dose in the energy ranges of 20 - 200 kVp X-rays (22). Optical density and dose radiation of this film has a linear relationship. The size of film used for dosimetry was 18 $\times$ 24 cm. Each film was placed in a specific packet composed of three different layers for protection against light and humidity.

In the first step, the film calibration curve was obtained by using the analogue radiology machine Varian-A-192 tube. The machine calibration curve as a function of kVp and mAs is derived by MATLAB software based on dose values measured in various kVp and mAs by the associated company. Then film response relative to radiation exposure is measured and calculated by the given specific dose with 0.5 mGy to 15 mGy exposure on discrete sections of the film. After processing, the films were scanned by Microtek-9800 XL scanner, and the film calibration curve was acquired by an in-house MATLAB software (22). In order to produce an equal condition for calibration setting, the film was placed at 100 cm distance of the tube under a 2 cm Plexiglass sheet.

Dosimetry was performed with a CBCT Soredex Cranex 3D device. Regarding the capability of manual setting, the

mA was considered as a varying factor and then scans were performed in the usual conditions of dental imaging of adults at 90kVp.

We specified the situation of the mandible, parotid and submandibular glands on two adjacent slices on the phantom based on the atlas of anatomy. Then, the films were placed between the two slices anatomically compatible with the desired organs (Figure 3).

The total of six CBCT scans were obtained, with 2, 4, 6, 8, 10 and 12 mA at 90 kVp. For all these measurements as a routine procedure, gantry was rotated around the phantom in 180 degree arc in the counter clockwise (CCW) direction. For every value of mA, measurements were repeated three times. The films were placed between the two slices anatomically compatible with the desired organs (Figure 3). These values of 6, 8 and 10 milliamperage are commonly used for adult dental scans. After processing and developing of the films, each one was scanned by a Microtek-9800 XL film scanner. This scanner has the capability of film scans with large sizes. All the images were saved in TIF format to keep the maximum information of the films. Using calibration curve of the film (Figure 4), the absorbed dose of each point was calculated by an in-house MATLAB software.

Finally, distribution of absorbed doses and isodose curves were obtained. The average values of three values of absorbed dose for each organ and the standard deviation were also calculated with MATLAB software. We performed a Tukey-Kramer (Tukey's W) multiple comparison analysis of ANOVA test using SPSS-20 software (IBM SPSS Statistics for Windows, Version 20.0. Armonk, NY: IBM Corp) used for evaluating the relationship between absorbed dose and mA at each part of the dentomaxillofacial area.

4. Results

Table 1 illustrates the dose for each part selected on the phantom and Table 2 shows the ratio of average doses at 2, 4, 6, 8 and 10 mA settings to dose at 12 mA setting and 90 kVp. In addition, P value was calculated between absorbed dose related to every paired mAs in each organ. Also, Pearson coefficient was calculated for any of organs between for each value of mAs and its related absorbed dose. Isodose curves obtained by MATLAB software of 90 kVp, 6 mA and field size 6 × 4 is demonstrated in Figure 5.

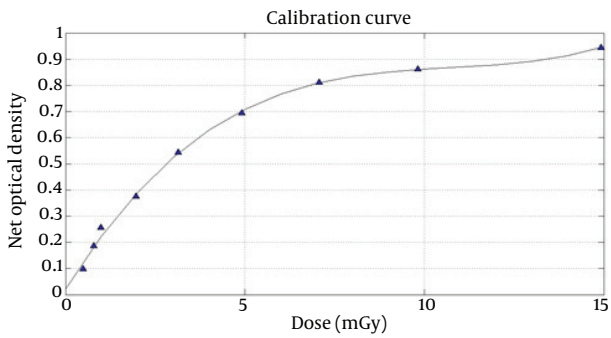

Figure 4. Calibration curve of the film

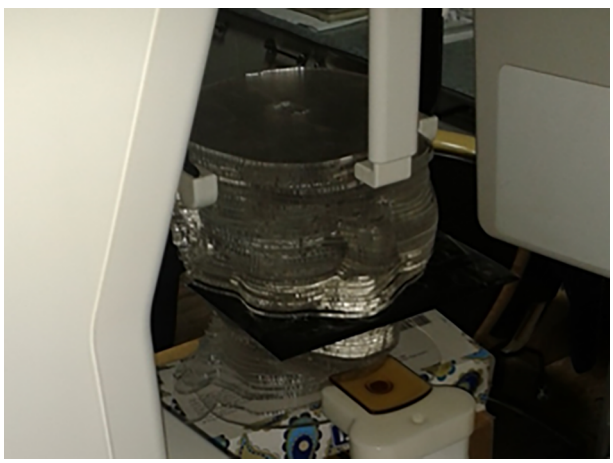

Figure 3. The film was placed between the two slices anatomically compatible with the desired organs.

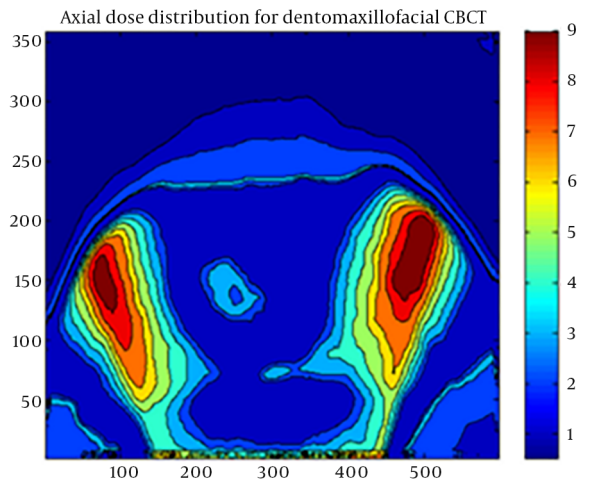

Figure 5. Isodose curves for the 90 kVp, 6 mA and field size 6 × 4. The color codes represent dose distributions in different parts in mGy.

Table 1. Doses of Different Parts at 2, 4, 6, 8, 10 and 12 mA with 90 kVp

Scanned area	Average dose (mGy)						P value for every paired mAs	Correlation coefficient between mAs and dose
	2 mA	4 mA	6 mA	8 mA	10 mA	12 mA		
Right mandible	2.95	3.60	5.76	8.22	10.67	12.55	< 0.05	0.99
Left mandible	2.87	3.27	5.53	7.96	10.33	12.19	< 0.05	0.99
Right parotid	1.88	2.59	4.04	5.91	8.19	10.23	< 0.05	0.99
Left parotid	1.86	2.42	3.85	5.08	7.35	9.89	< 0.05	0.99
Right submandibular	1.78	2.50	3.95	5.80	7.9	9.98	< 0.05	0.99
Left submandibular	1.98	2.50	3.80	5.44	7.43	9.15	< 0.05	0.99

Abbreviations: mA, milliamperage; mGy, milligray.

Table 2. Average Dose Ratio at 2, 4, 6, 8, 10 mA to Dose at 12 mA Setting and 90 kVp

Scanned area	Average dose ratio					
	2 mA	4 mA	6 mA	8 mA	10 mA	12 mA
Right mandible	0.23	0.29	0.46	0.65	0.84	1.00
Left mandible	0.23	0.27	0.45	0.65	0.85	1.00
Right parotid	0.18	0.25	0.39	0.58	0.80	1.00
Left parotid	0.19	0.24	0.39	0.51	0.74	1.00
Right submandibular	0.18	0.25	0.39	0.58	0.79	1.00
Left submandibular	0.22	0.27	0.41	0.59	0.81	1.00

Abbreviation: mA, milliamperage.

5. Discussion

As shown in Table 1, increasing mA has resulted in an increase in the average absorbed dose delivered to each part. As it has been represented in Table 1, for all scanned areas, the increase of absorbed dose by increase of mA is meaningful for 95% confidence. Correlation coefficient between mA and absorbed dose for each value of mA related to any of organs is positive and it shows that there is a positive correlation between mA and absorbed dose for any organ in each value of mA. The maximum and the minimum absorbed dose is placed in the area related to the right mandible and the left submandibular gland, respectively. By changing the value of mA from 2 to 12, absorbed dose varied significantly, with a maximum 5.44-fold variation between the highest and lowest dose for the right parotid.

In this study, average variations of absorbed dose versus mA in CBCT Soredex Cranex 3D for different parts of jaw and face have been evaluated. As mentioned in the previous sections, in order to meet ALARA principle, it is necessary to exist a balance between dose and image quality. Previous studies show that low exposure settings of radiation factors in medical CT scan units might result in similar image quality to higher exposure settings (5-10).

This study shows that increase in milliamprege of the device from 2 to 12 mA in routine condition in which kVp is set on 90, shows a meaningful increase in the absorbed dose. This result is in conformity with a study conducted by Palomo et al. (12). In both studies a considerable dose reduction was obtained by low exposure setting (12).

Kwong et al. evaluated the image quality of CT scan of the maxillary sinus in 40 patients with constant kVp and varying mA and concluded that there was a significant difference between absorbed dose of low and high exposure settings (5) which is in agreement to this study.

In this study, the absorbed dose received to the area related to the right parotid gland had the maximum value among other salivary glands. These results are completely in agreement with the study performed by Khajooei-Fard et al. in which the averaged absorbed dose delivered to the right and left parotid gland was 8.1 mGy and 7.3 mGy respectively with 90 kVp and 6 mA (23). In addition, according to our results, increasing the average absorbed dose in the right mandible was in good agreement with values obtained by Palomo et al. (12).

To conclude, with adherence to the previous studies, setting the radiation factors such as mA and kV in order to reach an optimization between absorbed dose and image quality is still considered as a controversial issue. In

this study, a special phantom was developed that enabled one to perform direct film dosimetry inside the simulated organs. The phantom had similar radiological properties to one specific patient with the average size. In this project, it was found that there was a significant relationship between the increase of milliamperage and increase of absorbed dose of different parts of the maxillafacial area including submandibular glands, parotid glands and mandibular bone imaged by CBCT Sordex Cranex 3D unit. Therefore, regarding the significant effect of lower exposure settings on absorbed dose reduction, evaluation of image quality by varying exposure factors is strongly recommended in future studies in order to optimize exposure settings to accomplish the goal of preserve image quality.

Footnotes

Authors' Contributions: Study concept and design: Zahra Alirezaei, Keyvan Jabbari and Mohammadbagher Tavakoli; experiments: Zahra Alirezaei, Tohid Dehghani and Mojdeh Mehdizadeh; analysis and interpretation of data: Zahra Alirezaei and Tohid Dehghani; MATLAB software analysis: Zahra Alirezaei and Nafiseh Berenjkoob; drafting of the manuscript: Zahra Alirezaei and Keyvan Jabbari; critical revision of the manuscript for important intellectual content: Keyvan Jabbari; statistical analysis: Zahra Alirezaei and Reihane Faraji.

Financial Disclosure: There are no financial interests related to the material in the manuscript.

Funding/Support: Funding of this project was provided by Isfahan University of Medical Sciences (Grant No: 373983).

References

1. Scarfe WC, Farman AG, Sukovic P. Clinical applications of cone-beam computed tomography in dental practice. *J Can Dent Assoc*. 2006;**72**(1):75–80. [PubMed: 16480609].
2. Mozzo P, Procacci C, Tacconi A, Martini PT, Andreis IA. A new volumetric CT machine for dental imaging based on the cone-beam technique: Preliminary results. *Eur Radiol*. 1998;**8**(9):1558–64. [PubMed: 9866761].
3. Yamamoto K, Ueno K, Seo K, Shinohara D. Development of dentomaxillofacial cone beam X-ray computed tomography system. *Orthod Craniofac Res*. 2003;**6 Suppl 1**:160–2. [PubMed: 14606550].
4. Elefteriadis JN, Athanasiou AE. Evaluation of impacted canines by means of computerized tomography. *Int J Adult Orthodon Orthognath Surg*. 1996;**11**(3):257–64. [PubMed: 9456629].
5. Kwong JC, Palomo JM, Landers MA, Figueroa A, Hans MG. Image quality produced by different cone-beam computed tomography settings. *Am J Orthod Dentofacial Orthop*. 2008;**133**(2):317–27. doi: 10.1016/j.ajodo.2007.02.053. [PubMed: 18249300].
6. Schulze D, Heiland M, Schmelzle R, Rother UJ. Diagnostic possibilities of cone-beam computed tomography in the facial skeleton. *Int Congr Ser*. 2004;**1268**:1179–83. doi: 10.1016/j.ics.2004.03.286.
7. Schulze D, Heiland M, Thurmann H, Adam G. Radiation exposure during midfacial imaging using 4- and 16-slice computed tomography, cone beam computed tomography systems and conventional radiography. *Dentomaxillofac Radiol*. 2004;**33**(2):83–6. doi: 10.1259/dmfr/28403350. [PubMed: 15313998].
8. Ludlow JB, Ivanovic M. Comparative dosimetry of dental CBCT devices and 64-slice CT for oral and maxillofacial radiology. *Oral Surg Oral Med Oral Pathol Oral Radiol Endod*. 2008;**106**(1):106–14. doi: 10.1016/j.tripleo.2008.03.018. [PubMed: 18504152].
9. Pauwels R, Beinsberger J, Collaert B, Theodorakou C, Rogers J, Walker A, et al. Effective dose range for dental cone beam computed tomography scanners. *Eur J Radiol*. 2012;**81**(2):267–71. doi: 10.1016/j.ejrad.2010.11.028. [PubMed: 21196094].
10. Silva MA, Wolf U, Heinicke F, Bumann A, Visser H, Hirsch E. Cone-beam computed tomography for routine orthodontic treatment planning: A radiation dose evaluation. *Am J Orthod Dentofacial Orthop*. 2008;**133**(5):640 e1–5. doi: 10.1016/j.ajodo.2007.11.019. [PubMed: 18456133].
11. Pauwels R, Silkosessak O, Jacobs R, Bogaerts R, Bosmans H, Panmekiate S. A pragmatic approach to determine the optimal kVp in cone beam CT: Balancing contrast-to-noise ratio and radiation dose. *Dentomaxillofac Radiol*. 2014;**43**(5):20140059. doi: 10.1259/dmfr.20140059. [PubMed: 24708447]. [PubMed Central: PMC4082271].
12. Palomo JM, Rao PS, Hans MG. Influence of CBCT exposure conditions on radiation dose. *Oral Surg Oral Med Oral Pathol Oral Radiol Endod*. 2008;**105**(6):773–82. doi: 10.1016/j.tripleo.2007.12.019. [PubMed: 18424119].
13. Farman AG. ALARA still applies. *Oral Surg Oral Med Oral Pathol Oral Radiol Endod*. 2005;**100**(4):395–7. doi: 10.1016/j.tripleo.2005.05.055. [PubMed: 16182157].
14. Martin CJ, Sutton DG, Sharp PF. Balancing patient dose and image quality. *Appl Radiat Isot*. 1999;**50**(1):1–19. [PubMed: 10028625].
15. Brenner DJ. Effective dose: A flawed concept that could and should be replaced. *Br J Radiol*. 2008;**81**(967):521–3. doi: 10.1259/bjr/22942198. [PubMed: 18443016].
16. Martin CJ. Effective dose: How should it be applied to medical exposures? *Br J Radiol*. 2007;**80**(956):639–47. doi: 10.1259/bjr/25922439. [PubMed: 17646189].
17. Valentin J. The 2007 recommendations of the International Commission on Radiological Protection. ICRP publication 103. *Ann ICRP*. 2007;**37**(2-4):1–332. doi: 10.1016/j.icrp.2007.10.003. [PubMed: 18082557].
18. Thilander-Klang A, Helmrot E. Methods of determining the effective dose in dental radiology. *Radiat Prot Dosimetry*. 2010;**139**(1-3):306–9. doi: 10.1093/rpd/ncq081. [PubMed: 20211918].
19. Huda W, Sandison GA. Estimation of mean organ doses in diagnostic radiology from Rando phantom measurements. *Health Phys*. 1984;**47**(3):463–7. [PubMed: 6500950].
20. Winslow JF, Hyer DE, Fisher RF, Tien CJ, Hintenlang DE. Construction of anthropomorphic phantoms for use in dosimetry studies. *J Appl Clin Med Phys*. 2009;**10**(3):2986. [PubMed: 19692982]. [PubMed Central: PMC5720556].
21. Alirezaei Z, Jabbari K, Tavakkoli MB, Dehghani T, Mahdavi H. [Design and construction of anthropomorphic phantom, using a CT-Scan of a particular patient for CT-Scan dosimetry studies]. *J Isfahan Med Sch*. 2015;**33**(323):125–33. Persian.
22. Berenjkoub N, Tavakoli MB, Jabbari K, Monadi S, Rahnama HR. [Investigation of dose distributions of computed tomography with cylindrical polymethyl methacrylate (PMMA) phantoms]. *J Isfahan Med Sch*. 2015;**32**(309):1918–32. Persian.
23. Khajooei-Fard R, Tavakoli MB, Mahdizadeh M, Hasanzadeh A. [Comparison of the absorbed doses of eyes, thyroid and parotid glands in dental cone beam computed tomography (CBCT) and panoramic examinations using cranex® 3D]. *J Isfahan Med Sch*. 2016;**34**:1151–9. Persian.